Biosensors and Bioelectronics 169 (2020) 112573

Contents lists available at ScienceDirect

Biosensors and Bioelectronics

journal homepage: http://www.elsevier.com/locate/bios

Impedimetric immunosensor for rapid and simultaneous detection of chagas and visceral leishmaniasis for point of care diagnosis

Taís Aparecida Reis Cordeiro [a], Helen Rodrigues Martins [b], Diego Leoni Franco [c], Fred Luciano Neves Santos [d], Paola Alejandra Fiorani Celedon [e], Vinícius Lopes Cantuária [b], Marta de Lana [f], Alexandre Barbosa Reis [f], Lucas Franco Ferreira [a,*]

[a] Institute of Science and Technology, Laboratory of Electrochemistry and Applied Nanotechnology, Federal University of the Jequitinhonha and Mucuri Valleys, Diamantina, Minas Gerais, Brazil
[b] Department of Pharmacy, Federal University of the Jequitinhonha and Mucuri Valleys, Diamantina, Minas Gerais, Brazil
[c] Institute of Chemistry, Group of Electrochemistry Applied to Polymers and Sensors, Laboratory of Electroanalytical Applied to Biotechnology and Food Engineering, Federal University of Uberlândia, Patos de Minas, Minas Gerais, Brazil
[d] Advanced Laboratory of Public Health, Gonçalo Moniz Institute (IGM), FIOCRUZ-BA, Salvador, Bahia, Brazil
[e] Molecular Biology Institute of Paraná, Curitiba, Paraná, Brazil
[f] Department of Clinical Analysis, School of Pharmacy, Federal University of Ouro Preto, Ouro Preto, Minas Gerais, Brazil

ARTICLE INFO

Keywords:
Chagas
Visceral leishmaniasis
Dual detection
Impedimetric immunosensor
Electropolymerization

ABSTRACT

In this work, a dual detection system based on an impedimetric immunosensor was developed for the first time for the simultaneous detection of anti-*Trypanosoma cruzi* and anti-*Leishmania infantum* antibodies in human and dog serum samples. The IBMP 8.1 and rLci1A/rLci2B recombinant antigens were immobilized over the surface of dual screen-printed carbon electrodes (W1 and W2) modified with poly (4-hydroxyphenylacetic acid). Under optimized conditions, the immunosensor recognized specific interactions for anti-T. *cruzi* antibodies up to a dilution of 1:10,240 and for anti-L. *infantum* up to 1:5120 in canine serum samples. Relative standard deviation (RSD) values of 2.8% for W1 and 3.6% for W2 were obtained for T. *cruzi* (W1) and *L. infantum* antigen (W2) samples in three different electrodes for 3 days (n = 9). The immunosensor was stored at 4 °C for 8 weeks, with activity retention of 70.2% in W1 and 78.2% in W2. The results using the recombinant proteins revealed that all antigens discriminated between negative and positive samples ($p < 0.0001$) in both dog and human groups, as well as no cross-reactivity could be detected among sera with other infections. With this approach, immunosensor-based diagnostic tests achieved 100% accuracy, suggesting that the antigens are eligible to enter Phase-II studies.

1. Introduction

Leishmaniasis and Chagas disease are important endemic diseases. Leishmaniasis is caused by protozoa of the genus *Leishmania* and classified as one of the main neglected diseases (Steverding, 2017). In Brazil, leishmaniasis can be divided into two different classes according to the type of *Leishmania* species and the immune response developed by the individual infected: Cutaneous leishmaniasis (CL) and visceral leishmaniasis (VL). Of these, VL has the highest mortality, and the number of cases is directly correlated with the economic situation of the region (Duthie et al., 2018; Okwor and Uzonna, 2016; Reguera et al., 2019; Selvapandiyan et al., 2019). Chagas disease (CD) is an endemic chronic infection caused by the flagellated protozoan *Trypanosoma cruzi*, with symptomatic forms in about 30% of people infected (Dutra et al., 2009). Despite the efforts to control transmission, there is still a range of infected individuals who need fast diagnosis and care (Coura, 2015; Pérez-Molina and Molina, 2018).

Serological tests are most frequently used for the diagnosis of these diseases in Brazil. When comercial diagnose kits, employing crude soluble antigens are used, the execution is time-consuming and shows cross-reactions due to the genetic similarity of the parasites that causes these infections (da Silva et al., 2013; Santos et al., 2016). Consequently, in endemic areas, the safe definition of the diagnosis can be complex in cases of co-infection in humans or dogs and with the risk of

* Corresponding author.
E-mail address: lucas.franco@ict.ufvjm.edu.br (L.F. Ferreira).

https://doi.org/10.1016/j.bios.2020.112573
Received 2 June 2020; Received in revised form 25 August 2020; Accepted 28 August 2020
Available online 29 August 2020

cross-reactions and/or individuals with little reactivity or with low antibody titers (Matos et al., 2015; Srivastava et al., 2011). In this sense, studies that seek to identify the simultaneous infection of *T. cruzi* and *L. infantum* in humans and dogs become necessary for the correct identification and differentiation of these species (Daltro et al., 2019). This situation has been rarely evaluated, but is of utmost importance for correct diagnosis without false-positive/negative results. Particularly in leishmaniasis, a correct diagnosis avoids unnecessary sacrifices of infected dogs, as well as risks represented by infected dogs judged as false negatives and able to infect vectors (Ferreira et al., 2014).

In recent years, electrochemical immunosensors have gained considerable interest as bioanalytical devices, particularly for the diagnosis and monitoring of diseases (Aydin and Sezgintürk, 2017; Chinnadayyala et al., 2019; Dai et al., 2019; Zhang et al., 2018). Electrochemical impedance spectroscopy (EIS) has been used as a label-free, sensitive, and powerful technique to study surface phenomena and changes in bulk properties. As most antibodies and antigens are electrochemically inert, EIS has been developed to provide direct detection of immunospecies, thereby representing a nondestructive means for the characterization of the electrical properties of biological interfaces (Katz and Willner, 2003). The biological component is immobilized on the working electrode, and the interaction with an analyte molecule is detected (Chen et al., 2008; Lisdat and Schäfer, 2008).

Recently, we reported the preparation of an electrochemical immunosensor based on modified screen-printed gold electrodes for the diagnosis of canine visceral leishmaniasis. The developed EIS immunosensor demonstrated suitable performance for the detection of *L. infantum* antibodies in sera samples, illustrating its potential for clinical and epidemiological purposes. However, the developed biosensor employed crude antigens that can fail in terms of sensitivity and specificity and cross-react with other pathogens (Cordeiro et al., 2019).

Herein, we propose the development of an impedimetric immunosensor for the simultaneous diagnosis of CD and VL, aiming to establish perspectives for improvements in the diagnosis of both diseases using the IBMP 8.1 and rLci1A/rLci2B recombinant antigens with an accurate performance for the individual diagnosis of CD and VL, respectively, as previously demonstrated (Borja et al., 2018; Daltro et al., 2019; de Oliveira et al., 2015; de Souza et al., 2012; Del-Rei et al., 2019; Dopico et al., 2019; Fraga et al., 2014; Ker et al., 2019; Leony et al., 2019; Santos et al., 2016, 2017a; 2017b).

Such methodology is extremely promising for the diagnosis of these and other infections, demonstrating higher sensitivity than the traditional tests used, besides the possibility of a faster and real-time analysis with perspectives for application in endemic areas. The present study brings innovations to this scientific area since there are no previous studies reported in the literature related to the simultaneous detection of CD and VL using a dual screen-printed carbon electrode. Thereforem, our results present a significant contribution to the improvement of the diagnosis.

2. Materials and methods

2.1. Reagents and apparatus

We used the following chemicals: 4-hydroxyphenylacetic acid (4-HPA) monomer (99%, Alfa Aesar, Haverhill, MA, USA); $HClO_4$ (70%, Sigma-Aldrich, São Paulo, São Paulo, Brazil), $K_3Fe(CN)_6$ and $K_4Fe(CN)_6$ (99%, Sigma-Aldrich, São Paulo, São Paulo, Brazil), KCl (99%, Vetec, Duque de Caxias, Rio de Janeiro, Brazil), 4-(2-hydroxyethyl)piperazine-1-ethanesulfonic acid (HEPES), purchased from Sigma-Aldrich Chemical (St. Louis, MO, USA). Ethylenediaminetetraacetic acid (EDTA), NaCl, and HCl were purchased from Isofar (Rio de Janeiro, Brazil). Tween 20 (surfactant P20) 0.005% and KOH were obtained from NEON (São Paulo, Brazil).

The HEPES buffer saline containing EDTA and polysorbate 20 (HBS-EP) were obtained by mixing solutions of 10.0 mmol L^{-1} HEPES pH 7.4, 3.0 mmol L^{-1} EDTA pH 8.0, 150.0 mmol L^{-1} NaCl, and 0.005% surfactant P20. All solutions were prepared using deionized water (18.2 MΩ. cm) from a Master System MS2000 of Gehaka, and all chemicals were of analytical grade and used as received.

Electrochemical impedance spectroscopy (EIS) and cyclic voltammetry (CV) were performed with a potentiostat/galvanostat from Autolab® model, PGSTAT204 equipped with FRA32M and BIPOT modules coupled to a computer with the Nova 2.1 software. The EIS analyses were carried out in 5.0 mM K_4 $[Fe(CN)_6]/K_3$ $[Fe(CN)_6]$ solution containing 0.1 M KCl. The frequency range varied between 100 kHz and 10 mHz, the amplitude of sinusoidal excitation was 10.0 mV, and the open circuit potential (OCP) was applied. An equivalent circuit that best fits the system proposed was used to analyze the experimental data. Fit and simulation procedures were performed using the software Nova 2.1.4.

The dual screen-printed carbon electrode (dSPCE) model DRP-X1110 (Lot. E0019539) was purchased from DropSens (Llanera, Asturias, Spain). Each chip has two elliptic carbon working electrodes, W1 and W2 (each with an area of 6.3 mm^2), a U-shaped carbon counter electrode (19.8 mm^2 and 1.0 mm wide) that equally surrounds both electrodes, and a silver pseudo-reference electrode onto a ceramic base.

2.2. Production of soluble recombinant antigens of T. cruzi and L. infantum

The *T. cruzi*-chimeric antigen IBMP 8.1 was obtained according to the methods reported by Santos et al. (2016a). Briefly, the *T. cruzi* recombinant gene was optimized for *Escherichia coli* expression and synthesized by a commercial supplier (GenScript, Piscataway, NJ, USA). The purchased synthetic gene the pUC57 was subcloned in-house into the pET28a *E. coli* expression vector. *Escherichia coli* BL21-Star (DE3) was grown in LB medium, and the recombinant antigen was obtained as a soluble protein after induction with 0.5 mM of isopropyl-β-D-1-thiogalactopyranoside (IPTG). The IBMP 8–1 was purified by both affinity and ion-exchange chromatography and quantified using a fluorimetric assay (Qubit 2.0, Invitrogen Technologies, Carlsbad, CA, USA).

The proteins rLci1A and rLci2B were cloned in pRSET B and pBK-CMV, respectively. *Escherichia coli* BL21 (DE3)/pLysS was transformed with pRSET plasmids containing the Lci1A or Lci2B *L infantum* gene insert. Recombinant protein expression was induced by the addition of 1 mM isopropyl-β-D-thiogalactopyranoside. After the expression step, the rLci1A and rLci2B proteins were purified by affinity chromatography, as previously described by de Souza et al. (2012). An equimolar mixture of the rLci1A and rLci2B recombinant antigens was used for immunosensor development.

2.3. Immunosensor fabrication and working principle

Scheme 1shows a typical dSPCE and the sequence of surface modification layer-by-layer for the development of the immunosensor platform for two different antigen sets.

Before electropolymerization, the dSPCE was electrochemically cleaned by 5 cyclings within the potential range −0.3 to +1.20 V at a scan rate of 50 mV s^{-1} in 0.50 M $HClO_4$ aqueous solution. Then, the electrode was rinsed with water and dried N_2. Electropolymerization on the electrode surface was conducted by CV, cycling the potential from 0.0 to +1.20 V. The 4- HPA solution at 2.50 mM was prepared in 0.50 M $HClO_4$ aqueous solution and used as the supporting electrolyte. The number of potential cycles, such as 5, 10, 15, and 20 cycles, at 50 mV s^{-1} was investigated for the application of this electrochemical platform in the development of an impedimetric immunosensor.

After electropolymerization, the electrodes coated by poly (4-HPA) – poly (4-HPA)/dSPCE – were washed with deionized water and dried under N_2 (g) flow. Afterward, one drop (2 μL) of *T.cruzi* recombinant

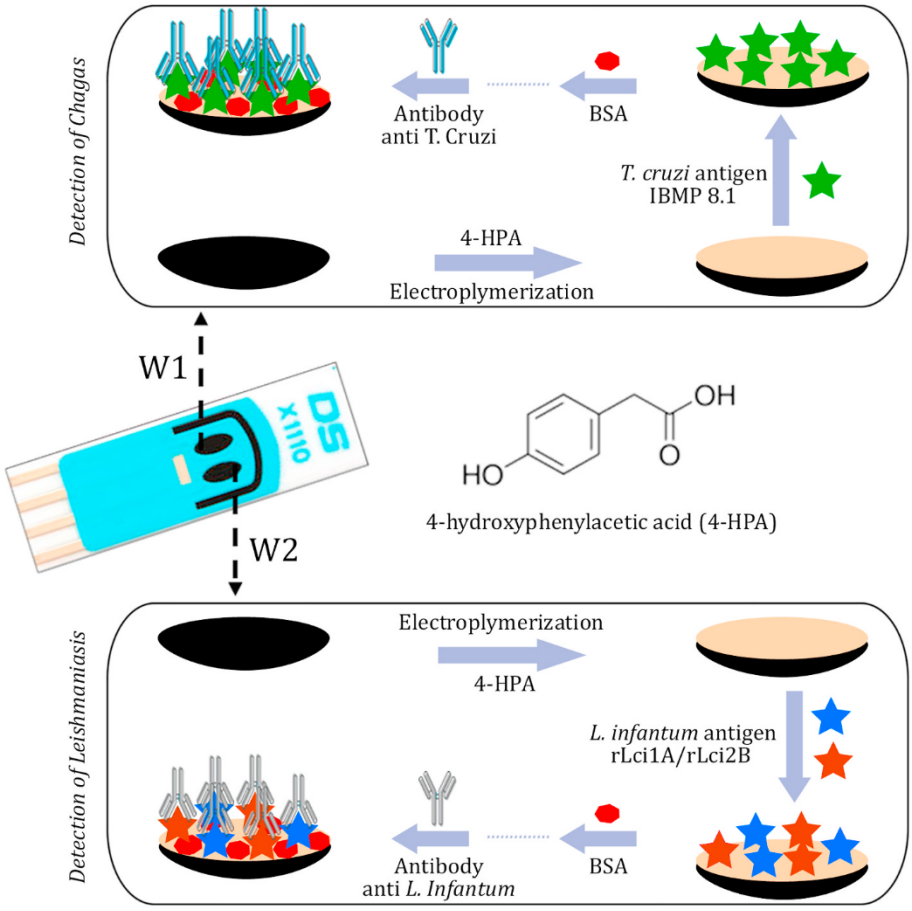

Scheme 1. Representation of dSPCE and sequence of surface modification in the preparation of the immunosensor platform.

antigen was immobilized on the W1. The same thing was peformed with another 2 μL of *L.infantum* recombinant antigen on W2. In this step, various concentrations of antigens were investigated, as well as different immobilization times of these antigens on the surface of poly (4-HPA)/dSPCE. To minimize non-specific binding, the potential remaining reactive site of the antigen was blocked with 1% BSA solution (prepared in HBS-EP buffer) and incubated at room temperature for 15 min (optimized). Prior to any reagent immobilization step, the electrode was washed with HBS-EP buffer solution. All experiments were performed in triplicate at room temperature (25 ± 2 °C) in non-humid conditions.

2.4. Detection of the immunoreaction and cross-reaction evaluation

After antigen immobilization, 30 canine sera were used to assess the ability of the sensor to detect specific targets and possible cross-reactions: 10 positive sera for visceral leishmaniasis (VL), 10 positive sera for Chagas disease (CD), and 10 negative sera for both infections. All sera were used as a pool of positive samples for VL or CD. Sera samples were tested in different dilutions (1:40, 1:80, 1:160, 1:320, 1:640, 1:1280, 1:2560, 1:5120, and 1:10240) in HBS-EP buffer, pH 7.4. The immunoreaction between immobilized antigen and antibody was essayed for different times (5, 10, 15, 20, 25, and 30 min). For serum dilution, a 2.0 μL sample was dropped over the working electrode surface; EIS readings were taken at each layer of the sensor construction and before and after antibody incubation. Subsequently, the R_{ct} value change upon incubation with each antigen concentration was calculated using the following equation:

$$\Delta R_{ct} = R_{ct}\ (\text{antibody, X dilution}) - R_{ct}\ (\text{immunosensor}) \quad (1)$$

2.5. Sample collections

All canine sera were previously tested through the serological assays from CD and VL infections by ELISA and/or indirect immunofluorescent-antibody (IFA) methods. Using previously collected anonymized human sera from *T. cruzi*-positive (n = 10) and -negative (n = 10) individuals and *T. cruzi*-positive (n = 10) and -negative (n = 10) dogs, the immunosensor performance and reactivity index (RI) distributions of IBMP-8.1 recombinant protein were assessed. For the rLci1A/rLci2B antigens, similar analyses were carried out employing human and canine *L. infantum chagasic*-positive and -negative samples (10 serum samples of each group). All sera were obtained from endemic settings from Minas Gerais (MG) and stored in the biorepository of the Chagas Disease and Immunopathology Laboratory of the Federal University of Jequitinhonha and Mucuri Valleys (UFVJM).

In addition to these sera, 10 samples from patients with unrelated diseases, as previously defined by their serological or parasitological diagnoses (reference standard tests), were kindly provided by the Ezequiel Dias Foundation (FUNED; Belo Horizonte, MG/Brazil) and incorporated into the present sera sample set to evaluate cross-reactivity. The unrelated diseases evaluated included American cutaneous leishmaniasis (n = 2), Hepatitis B virus (n = 2), Human immunodeficiency virus (n = 2), Human T-cell lymphotropic virus (n = 2), and Toxoplasmosis (n = 2).

2.6. Statistical analysis

Data were analyzed using a scatter plot graphing software (GraphPad Prism version 8, San Diego, CA, USA). Continuous variables were

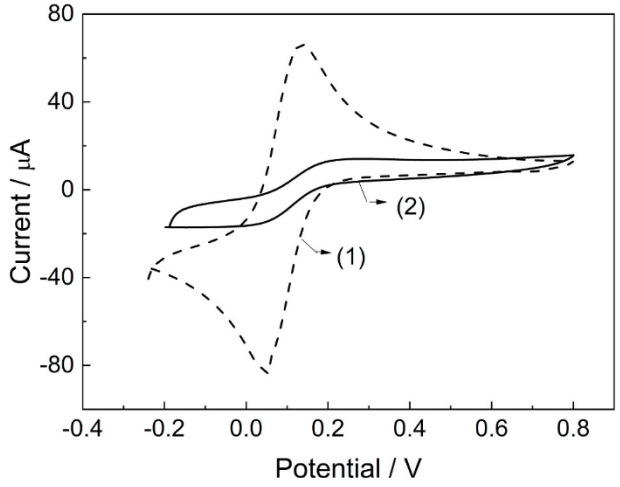

Fig. 1. Cyclic voltammograms obtained for bare dSPCE (Curve 1) and poly (4-HPA)/dSPCE (5 cycles) (Curve 2) in an aqueous solution containing $Fe(CN)_6^{3-/4-}$ (5.0 mmol L^{-1}) and KCl (0.1 mol L^{-1}) at scan rate of 100 mV s^{-1}.

determined as geometric mean ± standard deviation (SD), and the Shapiro-Wilk test was used to test data normality. When the assumed homogeneity was confirmed, Student's t-test was used; otherwise, Wilcoxon's signed-rank test was employed. A 5% level of significance was adopted for all statistical testing (P value < 0.05). Areas under the ROC curve (AUC) were calculated to evaluate the global accuracy for each IBMP antigen, which can be classified as low (0.51–0.61), moderate (0.62–0.81), elevated (0.82–0.99), or outstanding (1.0) (Swets, 1988). All results from the immunosensor were measured by the change of the charge transfer resistance ($\Delta R_{ct}/k\Omega$), with the corresponding reactivity index (RI) values calculated as $\Delta R_{ct}/k\Omega$ divided by CO. Results were interpreted as follows: positive ($RI \geq 1.0$), negative ($RI < 1.0$), and grey zone ($0.90 = RI \leq 1.10$). The *T. cruzi* and *L. infantum* recombinant antigen performance parameters were determined using a dichotomous approach and compared regarding sensitivity (Se), specificity (Sp), and accuracy (Ac). A 95% confidence interval (95% CI) was calculated to address the precision of the proportion estimates. The strength of the agreement between immunosensor methodology, using IBMP-8.1 or rLci1A/rLci2B, and the serologic sample profile established previously was assessed using Cohen's Kappa coefficient (κ) (Landis and Koch, 1977), interpreted as follows: poor ($\kappa = 0$), slight ($0.20 \leq \kappa > 0$), fair ($0.40 \leq \kappa > 0.20$), moderate ($0.60 \leq \kappa > 0.40$), substantial ($0.80 \leq \kappa > 0.60$), almost perfect ($1.0 < \kappa > 0.80$), or perfect ($\kappa = 1.0$). A flowchart (Appendix A: Fig. S1) and a checklist (Appendix A: Table S1) have been provided according to the Standards for Reporting of Diagnostic Accuracy Studies (STARD) guidelines (Cohen et al., 2016).

3. Results and discussion

3.1. Characterization of the platform

To evaluate the electron transfer property of the polymeric film adsorbed onto the dSPCE surface, cyclic voltammetry (CV) was carried out using $Fe(CN)_6^{3-/4-}$ as a redox probe. Fig. 1 shows the cyclic voltammograms for the bare dSPCE (Curve 1) and poly (4-HPA)/dSPCE in the presence of the redox probe (curve 2). A couple of reversible redox peaks characteristic of a diffusion-limited redox process was observed at the bare electrode. When the electrode was modified with poly 4-HPA (Curve 2), a decrease in the anodic and cathodic current peaks was observed, which indicates that the polymer acts as the inert electron and mass transfer blocking layer, hindering the diffusion of the redox probe toward to electrode surface.

Figure S2-A in Appendix A shows the Nyquist plots for the dSPCE and poly (4-HPA)/dSPCE in the presence of the redox probe. Data were simulated by a Randles circuit ($[R_s\ (Q_{dl}\ [R_{ct}W])$ for unmodified electrodes and a modified Randles circuit ($[R_s\ (Q_{dl}\ [R_{ct}W])\ (R_fQ_f)]$) for modified electrodes. The dSPCE show a small value for resistance of charge transfer ($R_{ct} = 0.407\ k\Omega \pm 0.064$). However, after the modification with 5 cycles, the poly (4-HPA)/dSPCE showed a higher value for resistance of charge transfer ($R_{ct} = 10.5\ k\Omega \pm 0.7$), which means that probe access to the electrode surface was hindered. The presence of material with resistive behavior may cover the active electrochemical area of the electrode, which explains the charge transfer resistance increase. On the other hand, this increase can also indicate the adsorption of anionic material, according to studies by Santos et al. (2019). In this way, occurs an electrostatic repulsion between the anionic redox probe and the polymeric film.

Figure S2-B in Appendix A shows the Nyquist plots obtained for the poly (4-HPA)/dSPCE platforms under the different numbers of potential cycles. The number of potential cycles has a direct influence on the film formation and its use for biomolecule immobilization.

We tested 5, 10, 15, and 20 deposition cycles, and the modified electrode surface was optimized regarding its permeability toward redox mediators. This was performed to avoid surface insulation and to ensure the presence of free –COOH groups for biomolecule immobilization (Santos et al., 2019). It should be noted that as the number of deposition cycles increased, the R_{ct} value also increased, and the film itself tends to a more capacitive behavior and shows a higher total resistance ($R_T = R_{ct} + R_f$), which can be related to the different thicknesses. The parameter values obtained through simulation, described in Appendix A (Table S2), show that a higher number of cycles led to lower values of Q_{dl}, suggesting thicker films. Moreover, the small values of Warburg impedance, for all cases, suggest that the surface morphology of the poly (4-HPA) is more flat than porous.

The number of cycles was evaluated in the immobilization of the *T. cruzi* antigen and *L. infantum* antigens (Appendix A: Table S3) and the detection of an immunoreaction of each molecule set with its specific

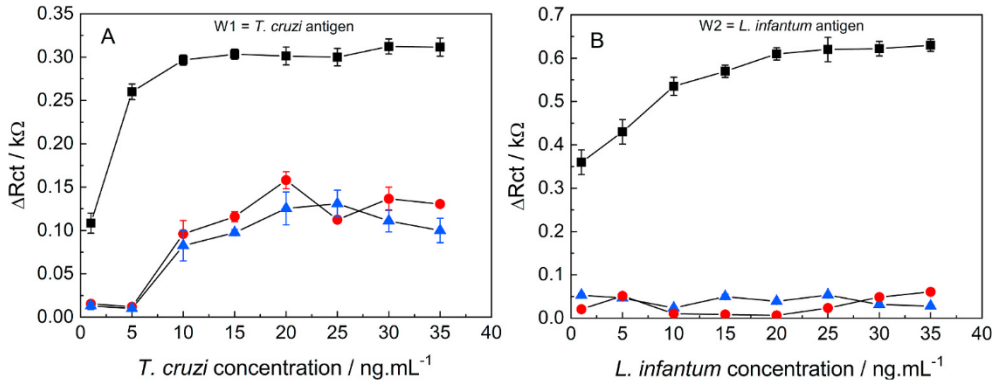

Fig. 2. (A) Dependence of ΔR_{ct} of the fabricated *T. cruzi* immunosensor (W1) on the concentration of antigens in the presence of the (■) specific target canine serum samples, (●) non-infected canine serum samples, and (▲) positive serum for *L. infantum*. (B) Dependence of ΔR_{ct} of the fabricated *L. infantum* immunosensor (W2) on the concentration of antigens in the presence of the (■) specific target canine serum samples, (●) non-infected canine serum samples, and (▲) positive serum for *T. cruzi*. All measurements were carried out in the KCl solution (0.1 mol L^{-1}) containing $Fe(CN)_6^{3-/4-}$ (5.0 mmol L^{-1}).

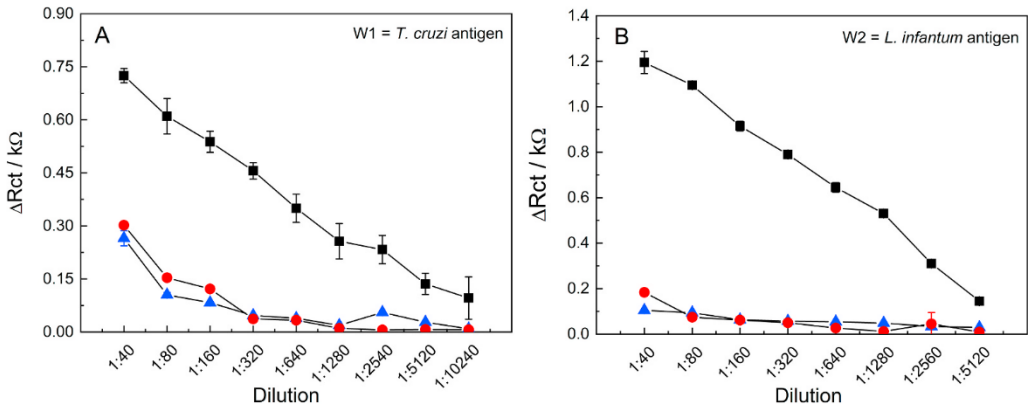

Fig. 3. A) ΔR_{ct} as a function of dilution factor of the (■) positive and (●) non-infected dogs and (▲) positive for visceral leishmaniasis in W1. B) ΔR_{ct} as a function of dilution factor of the (■) positive and (●) negative canine sera for visceral leishmaniasis and (▲) positive for Chagas in W2.

target. The poly (4-HPA)/dSPCE platform was sensitive to antigen immobilization and to the immunoreaction event in all investigated cycles. Subsequently, antibodies solutions were dipped over the modified surfaces, and the R_{ct} increased again, indicating the interaction between the antigen and the specific antibody. We did not observe a significant increase in ΔR_{ct} after 10 cycles of potential for W1 and after 15 cycles for W2. The poly (4-HPA)/dSPCE dual-platform formed with 15 scans was then selected for the subsequent experiments.

3.2. Optimization of T. cruzi and L. infantum antigen immobilization

The *T. cruzi* antigens (IBMP 8.1) were immobilized on electrode W1, while on electrode W2, *L. infantum* antigens (rLci1A/rLci2B) were immobilized; the impedance responses of W1 and W2 were recorded simultaneously. The *T. cruzi* (Appendix A: Fig. S3-A) and *L. infantum* (Appendix A: Fig. S3-B) antigen immobilization time was investigated from 5 to 30 min. The impedance decreased with increasing immobilization. Table S4 in Appendix A shows that the ΔR_{ct} incresed until na antigen immobilization time of 20 min for both antigens. After this, no major changes were observed, and ΔR_{ct} reached a plateau, which suggest that the antigen is interacting with the electrode surface that contains the negatively charged polymer. Thus, by antigen/polymer interaction, the values of charge transfer resistance decrease, as indicated in Section 3.1. This observation suggests that there were maximum reaction sites of antigen + BSA on the electrode surface within 20 min. As a result, the immobilization time of 20 min was selected for both antigens.

A wide range of concentration of antigens was immobilized on the poly (4-HPA)/dSPCE surface to determine optimum antigen concentration. The changes in R_{ct} values were plotted to observe the effects of changing antigen concentrations. As shown in Fig. 2, the ΔR_{ct} increased with the increasing concentration of the antigen on both electrodes. The immunosensor produced a response curve that increased until 10 ng/mL to the *T. cruzi* antigen concentration (W1 – Fig. 2A) and 20 ng/mL to the *L. infantum* antigen (W2 – Fig. 2B), with nonlinearity due to the onset of sensor saturation of the specific binding sites observed above these values. Therefore, a 10-ng mL^{-1} T. *cruzi* antigen concentration and a 20 ng mL^{-1} L. *infantum* antigen concentration in HBS-EP were chosen and used subsequently.

Usually, nonspecific adsorption is a significant problem in label-free immunosensing. Contrast experiments were performed to confirm that the observed impedance changes arise from specific interaction between Ag and Ab. After the immobilization of Ag and blocking with BSA, the electrode was exposed to non-specific antibodies. Fig. 2A shows plots that correspond to the resistance change (ΔR_{ct}) in the W1 in the presence of canine serum samples non-infected and infected by *L. infantum* at different concentrations of the *T. cruzi* antigen. Fig. 2B shows plots that correspond to the resistance change (ΔR_{ct}) in W2 in the presence of canine serum from non-infected and *T. cruzi* infection-positive samples at different *L. infantum* antigen concentrations. As shown in the figure, there was only a slight variation in the impedance in both cases. Such small changes of the electron-transfer resistance of the nonspecific adsorption are acceptable, and this observation indicates that the immunosensor had a good selectivity towards these serum samples.

3.3. Simultaneous response to anti-L. infantum and anti-T. cruzi antibodies

The incubation time for the antibodies over the immunosensor was investigated (5–30 min). As shown in Figure S4 (Appendix A), under and over the time of 20 min, there was no significant change in impedance (W1 and W2). A small ΔR_{ct} value was observed under 20 min as there was not enough time for antibody binding to the immobilized antigen. Also, a small ΔR_{ct} value was observed over 20 min, probably because all the active sites for Ab-Ag interactions were reached. For this reason, the reaction time of 20 min was selected for the immunosensor response.

Cross-reactions between patients with leishmaniasis and Chagas disease are common in conventional diagnosis tests, leading to false-positive results (Daltro et al., 2019; Santos et al., 2018a). After optimization, to evaluate the binding specificity of the sensor and the absence of cross-reactions, a pool of canine sera was employed: non-infected and positive for Chagas disease infection and positive for visceral leishmaniasis in W1; non-infected and positive for visceral leishmaniasis and positive Chagas disease in W2. Sera were prepared in different dilutions (1:40, 1:80, 1:160, 1:320, 1:640, 1:1280, 1:2560, 1:5120 and 1:10240) in HBS-EP buffer at pH 7.4. For each dilution, a different electrode was used, and it was added 2 μL of the sample at each immunosensor. The analyses were performed separately in W1 and W2, as shown in Fig. 3.

The dilution curves shown in Fig. 3A were obtained for W1. The immunosensor showed a linear relationship between R_{ct} variation and the dilution of the positive antibody. We observed a wide detection range and an excellent sensitivity of W1, the R_{ct} values decreased when the dilution increased, probably due to the lower antibody concentration in the sample. The addition of a negative control for Chagas infection and positive control for visceral leishmaniasis sera resulted in a lower response when compared with positive serum, indicating low cross-reactivity.

Similarly, Fig. 3B shows the dilution curves obtained for W2. The results indicate that the immunosensor presents high specificity for the detection of only the positive anti-*L. infantum* (no response to negative anti-*L. infantum*) and no cross-reactivity with Chagas disease-positive sera.

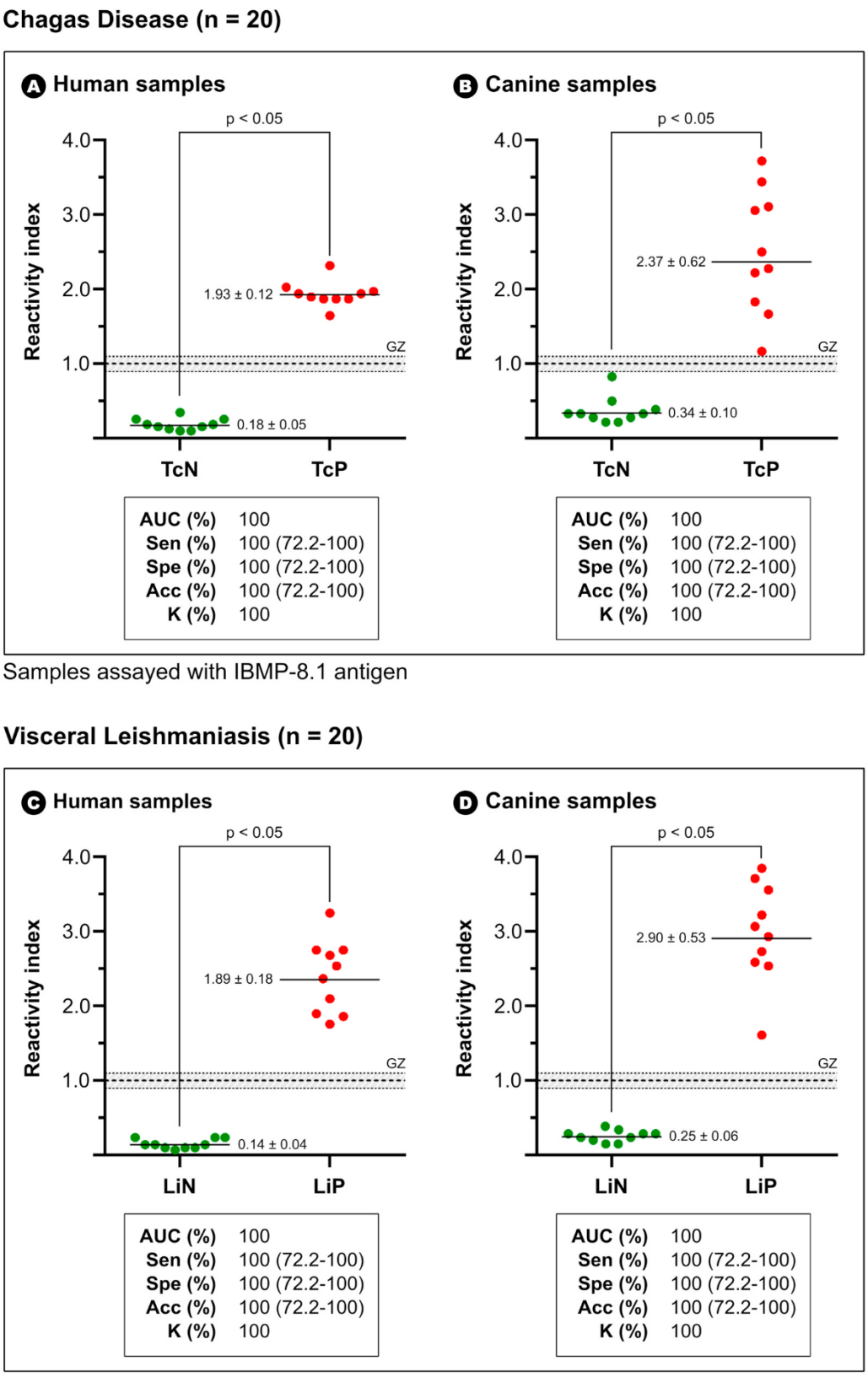

Fig. 4. Reactivity index obtained with human or canine serum samples from *T. cruzi*-positive (TcP), *T. cruzi*-negative (TcN), *L. infantum*-positive (LiP), and *L. infantum*-negative (LiN) individuals. The cut-off value is reactivity index = 1.0, and the shadowed area represents the grey zone (RI = 1.0 ± 0.10). Horizontal lines and numbers for each group of results represent the geometric means (±95% CI). AUC (Area Under Curve); Sen (Sensitivity); Spe (Specificity); Acc (Accuracy); K (Cohen's Kappa coefficient); GZ (Grey zone).

3.4. Selectivity, repeatability, and stability of the immunosensor

To confirm that the observed impedance changes were based on the specific interaction and to confirm the selectivity of the platform, the impedance immunosensor was incubated with a mixture of *T. cruzi* and *L. infantum* antibodies under the same experimental conditions. No significant decrease in impedance response was observed, suggesting that the specific interaction process between the antigen and the specific

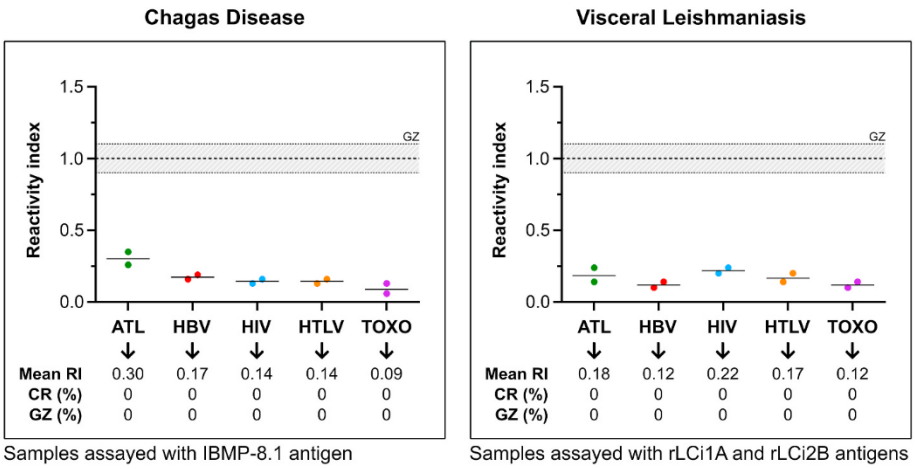

Fig. 5. Analysis of IBMP-8.1 or rLci1A/rLci2B cross-reactivity (CR) with human sera from individuals with unrelated diseases. The cut-off value is reactivity index = 1.0, and the shadowed area represents the grey zone (RI = 1.0 ± 0.10). Horizontal lines represent geometric means (95% CI), with the corresponding results shown below for each group. ATL (American tegumentary leishmaniasis); HBV (Hepatitis B virus); HIV (Human immunodeficiency virus); HTLV (Human T-cell lymphotropic virus); TOXO (Toxoplasmosis); GZ (Grey zone); RI (Reactivity index).

target might be driven by the binding through the specific sites of the recombinant proteins, which indicates that the immunosensor presents good selectivity and could be used to identify coinfections with these diseases (Appendix A: Figure S5-A). In the Brazilian Amazon, it is common to find patients with a coinfection of DC/VL, and therefore, it is important to obtain a correct interpretation of serological tests (Matos et al., 2015), which it is offered here.

The repeatability of the immunosensor was investigated. Samples of *T. cruzi* (W1) and *L. infantum* antigens (W2) were successfully detected in three different electrodes for 3 days (n = 9) under the optimized conditions, with relative standard deviation (RSD) values of 2.8% for W1 and 3.6% for W2 (Appendix A: Figure S5-B). This proves that a good reproducibility of the system was achievable for the simultaneous detection of antibodies anti-*T. cruzi* and anti-*L. infantum*.

An activity loss was detected after storage (8 weeks at 4 °C). The device retained 70.2% of this initial response in W1 and 78.2% in W2 (Appendix A: Figure S5-C). Long-term stability may be expected due to the stable attachment of the antigen molecules to the modified electrode surface, which can prevent the Ag from leaking out and has a minimal effect on the immunoreaction after storage. On the other hand, the loss can be related to the degeneration of the protein components of the biosensor since the antigens were adsorbed on the platform in the absence of any stabilizing or antioxidant agents. Modifications can be carried out in the Phase-II studies to improve stability as occurs with the immunochromatographic lateral-flow assay.

3.5. Preliminary studies of analytical performance

In the present study, we assessed the diagnostic performance of recombinant antigens for the detection of specific IgG anti-*T. cruzi* or *L. infantum* antibodies in sera from CD or VL-positive humans and dogs. After the development of the immunosensor and determination of the optimized conditions for the immunoassay, a preliminary evaluation was conducted to verify its performance for application in the simultaneous diagnosis of CD or VL. As shown in Fig. 4, the analysis of the samples at a dilution of 1:320 allows a clear separation between infected and not infected samples in both dog and human groups.

According to the AUC values, IBMP-8.1 and rLci1A/rLci2B antigens achieved outstanding values of global accuracy (1.0), indicating that they can efficiently distinguish positive from negative samples. Additionally, we found high sensitivity (100%), specificity (100%), and accuracy (100%) values, as well as a perfect agreement between the reference standard tests and the immunosensor. For the IBMP-8.1 antigen, these results are in agreement with previous data obtained by our group using ELISA (Del-Rei et al., 2019; Dopico et al., 2019; Leony et al., 2019; Santos et al., 2016a, 2017a, 2018b) or liquid microarray as diagnostic platforms (Santos et al., 2017b). For the rLci1A/rLci2B antigen, the impedimetric immunosensor showed results slightly higher than those obtained by our group, using the immunochromatographic rapid test prototype based on the dual path platform and flow cytometry serology (Fraga et al., 2014; Ker et al., 2019). Also, differences higher than 6.97 were seen between the RI signals (individual RI values are available in Appendix A: Table S5) from the positive and negative samples for all proteins, providing further evidence of their high discriminatory capability.

Considering the cross-reactivity assessment with sera from humans carrying unrelated pathogens (Fig. 5; individual RI values are available in Appendix A: Table S6), no sample tested positive with IBMP-8.1 or rLci1A/rLci2B. Similar results were found for IBMP-8.1, both using ELISA (Daltro et al., 2019; Del-Rei et al., 2019; Dopico et al., 2019; Leony et al., 2019; Santos et al., 2016a, 2017a, 2018b) and liquid microarray (Santos et al., 2017b). For rLci1A/rLci2B, the immunosensor again showed results higher than those obtained by our group, using the immunochromatographic rapid test prototype based on the dual path platform and flow cytometry serology (Fraga et al., 2014; Ker et al., 2019).

Our findings show total separation between infected and non-infected groups, as well as no cross-reactivity, could be detected among sera with other infections. This is extremely relevant since leishmaniasis represents an important source of false-positive results among conventional serological tests (Daltro et al., 2019). The successful development of a device with potential application in the simultaneous diagnosis of CD and VL in areas where *L. infantum* and *T. cruzi* are co-endemic would ultimately reduce diagnostic costs due to a significant reduction in the number of samples requiring reassaying. A comparison of some electrochemical biosensors reported for the detection of Chagas disease and visceral leishmaniasis is shown in Appendix A: Table S7.

4. Conclusions

In the present study, a dual detection system for the simultaneous detection of anti-*T. cruzi* and anti-*L. infantum* antibodies in serum samples was developed. The immunosensor was successfully applied in the analysis of antibodies against anti-T. cruzi in canine serum (up to 1:10240 dilution) and anti-Leishmania infantum serum (up to 1:5120 dilution). Good reproducibility and accuracy were obtained, meeting the prerequisites for disposable applications. It is predicted that the method can be used to construct a series of biosensors for the simultaneous determination of other species, allowing analysis of interactions in real-time and without needing markers. Phase-I studies are typically performed using a set of seronegative individuals and a set of seropositive individuals to evaluate whether the test can differentiate them (Irwig et al., 2002; Sackett and Haynes, 2002). The immunosensor

results using the IBMP-8.1 or rLci1A/rLci2B recombinant proteins revealed that all antigens appropriately discriminated between negative and positive samples ($p < 0.0001$), as demonstrated by ROC curve analysis (Appendix A: Figure S6). With this approach, immunosensor-based diagnostic tests achieved 100% accuracy, suggesting that the antigens are eligible to enter Phase-II studies.

CRediT authorship contribution statement

Taís Aparecida Reis Cordeiro: Conceptualization, Methodology, Investigation, Writing - original draft. **Helen Rodrigues Martins:** Conceptualization, Resources, Writing - review & editing. **Diego Leoni Franco:** Conceptualization, Writing - review & editing. **Fred Luciano Neves Santos:** Formal analysis, Resources, Writing - review & editing. **Paola Alejandra Fiorani Celedon:** Resources, Writing - review & editing. **Vinícius Lopes Cantuária:** Methodology, Investigation, Validation. **Marta de Lana:** Resources, Writing - review & editing. **Alexandre Barbosa Reis:** Resources, Writing - review & editing. **Lucas Franco Ferreira:** Conceptualization, Supervision, Project administration, Funding acquisition, Writing - review & editing.

Declaration of competing interest

The authors declare that they have no known competing financial interests or personal relationships that could have appeared to influence the work reported in this paper.

Acknowledgment

This work was supported by the Fundação de Amparo à Pesquisa do Estado de Minas Gerais (FAPEMIG), Brazil, (Project: APQ-03097-15).

Appendix A. Supplementary data

Supplementary data to this article can be found online at https://doi.org/10.1016/j.bios.2020.112573.

References

Aydin, E.B., Sezgintürk, M.K., 2017. Talanta 172, 162–170.
Borja, L.S., Coelho, L.B., de Jesus, M.S., de Queiroz, A.T.L., Celedon, P.A.F., Zachin, N.I.T., Silva, E.D., Ferreira, A.G.P., Krieger, M.A., Veras, P.S.T., Fraga, D.B.M., 2018. PLoS Neglected Trop. Dis. 12, e0006871.
Chen, X., Wang, Y., Zhou, J., Yan, W., Li, X., Zhu, J.J., 2008. Anal. Chem. 80, 2133–2140.
Chinnadayyala, S.R., Park, J., Abbasi, M.A., Cho, S., 2019. Biosens. Bioelectron. 143, 111642.
Cohen, J.F., Korevaar, D.A., Altman, D.G., Bruns, D.E., Gatsonis, C.A., Hooft, L., Irwig, L., Levine, D., Reitsma, J.B., de Vet, H.C.W., Bossuyt, P.M.M., 2016. BMJ Open 6, e012799.
Cordeiro, T.A., Gonçalves, M.V., Franco, D.L., Reis, A.B., Martins, H.R., Ferreira, L.F., 2019. Talanta 195, 327–332.
Coura, J.R., 2015. Mem. Inst. Oswaldo Cruz 110, 277–282.
da Silva, D.A., Madeira, M.F., Abrantes, T.R., Filho, C.J., Figueiredo, F.B., 2013. Vet. J. 195, 252–253.
Dai, L., Li, Y., Wang, Y., Luo, X., Wei, D., Feng, R., Yan, T., Ren, X., Du, B., Wei, Q., 2019. Biosens. Bioelectron. 132, 97–104.
Daltro, R.T., Leony, L.M., Freitas, N.E.M., Silva, Â.A.O., Santos, E.F., Del-Rei, R.P., Brito, M.E.F., Brandão-Filho, S.P., Gomes, Y.M., Silva, M.S., Donato, S.T., Jeronimo, S.M.B., Monteiro, G.R.G., Carvalho, L.P., Magalhães, A.S., Zanchin, N.I.T., Celedon, P.A.F., Santos, F.L.N., 2019. J. Clin. Microbiol. 57, e00762, 19.
de Oliveira, I.Q., Silva, R.A., Sucupira, M.V., da Silva, E.D., Reis, A.B., Grimaldi Jr., G., Fraga, D.B.M., Veras, P.S.T., 2015. Parasit. vectors 8, 45.
de Souza, C.M., Silva, E.D., Ano Bom, A.P., Bastos, R.C., Nascimento, H.J., da Silva Junior, J.G., 2012. Parasite Immunol. 34, 1–7.
Del-Rei, R.P., Leony, L.M., Celedon, P.A.F., Zanchin, N.I.T., Reis, M.G.D., Gomes, Y.M., Schijman, A.G., Longhi, S.A., Santos, F.L.N., 2019. PloS One 14, e0215623.
Dopico, E., Del-Rei, R.P., Espinoza, B., Ubillos, I., Zanchin, N.I.T., Sulleiro, E., Moure, Z., Celedon, P.A.F., Souza, W.V., da Silva, E.D., Gomes, Y.M., Santos, F.L.N., 2019. BMC Infect. Dis. 19, 251.
Duthie, M.S., Lison, A., Courtenay, O., 2018. Trends Parasitol. 34, 881–890.
Dutra, W.O., Menezes, C.A.S., Villani, F.N.A., da Costa, G.C., da Silveira, A.B.M., Reis, D.A., Gollob, K.J., 2009. Mem. Inst. Oswaldo Cruz 104, 208–218.
Ferreira, L.R., Kesper, N., Teixeira, M.M.G., Laurenti, M.D., Barbieri, C.L., Lindoso, J.A., Umezawa, E.S., 2014. Acta Trop. 131, 41–46.
Fraga, D.B.M., da Silva, E.D., Pacheco, L.V., Borja, L.S., de Oliveira, I.Q., Coura-Vita, W., Monteiro, G.R., Oliveira, G.G.S., Jerônimo, S.M.B., Reis, A.B., Veras, P.S.T., 2014. Parasites Vectors 7, 136.
Irwig, L., Bossuyt, P., Glasziou, P., Gatsonis, C., Lijmer, J., 2002. BMJ 324, 669–671.
Katz, E., Willner, I., 2003. Electroanalysis 15, 913–947.
Ker, H.G., Coura-Vital, W., Valadares, D.G., Aguiar-Soares, R.D.O., de Brito, R.C.F., Veras, P.S.T., Fraga, D.B.M., Martins-Filho, O.A., Teixeira-Carvalho, A., Reis, A.B., 2019. Appl. Microbiol. Biotechnol. 103, 8179–8190.
Landis, J.R., Koch, G.G., 1977. Biometrics 33, 159–174.
Leony, L.M., Freitas, N.E.M., Del-Rei, R.P., Carneiro, C.M., Reis, A.B., Jansen, A.M., Xavier, S.C.C., Gomes, Y.M., Silva, E.D., Reis, M.G., Fraga, D.B.M., Celedon, P.A.F., Zanchin, N.I.T., Dantas-Torres, F., Santos, F.L.N., 2019. PLoS Neglected Trop. Dis. 13, e0007545.
Lisdat, F., Schäfer, D., 2008. Anal. Bioanal. Chem. 391, 1555.
Matos, H.J., Pinto, A.Y.N., Miranda, A.M.M., Silva, F.L.C., Ramos, F.L.P., 2015. Rev. Pan-Amaz. Saude. 6, 65–68.
Okwor, I., Uzonna, J., 2016. Am. J. Trop. Med. Hyg. 94, 489–493.
Pérez-Molina, J.A., Molina, I., 2018. Lancet 391, 82–94.
Reguera, R.M., Pérez-Pertejo, Y., Gutiérrez-Corbo, C., Domínguez-Asenjo, B., Ordóñez, C., García-Estrada, C., Martínez-Valladares, M., Balaña-Fouce, R., 2019. Pure Appl. Chem. 91, 1385–1404.
Sackett, D.L., Haynes, R.B., 2002. BMJ 324, 539–541.
Santos, F.L.N., Celedon, P.A.F., Zanchin, N.I.T., Brasil, T.A.C., Foti, L., de Souza, W.V., Silva, E.D., Gomes, Y.M., Krieger, M.A., 2016a. PloS One 11, e0161100.
Santos, F.L.N., de Souza, W.V., Barros, M.S., Nakazawa, M., Krieger, M.A., Gomes, Y.M., 2016b. Am. J. Trop. Med. Hyg. 94, 1034–1039.
Santos, F.L.N., Celedon, P.A.F., Zanchin, N.I.T., de Souza, W.V., da Silva, E.D., Foti, L., Krieger, M.A., Gomes, Y.M., 2017a. PLoS Neglected Trop. Dis. 11, e0005433.
Santos, F.L.N., Celedon, P.A.F., Zanchin, N.I.T., Leitolis, A., Crestani, S., Foti, L., de Souza, W.V., Gomes, Y.M., Krieger, M.A., 2017b. J. Clin. Microbiol. 55, 2934–2945.
Santos, A.P.D., Carvalho, M.E.D., Meirelles, L.R., Andrade-Junior, H.F.D., 2018a. Rev. Soc. Bras. Med. Trop. 51, 665–669.
Santos, F.L.N., Campos, A.C.P., Amorim, L.D.A.F., Silva, E.D., Zanchin, N.I.T., Celedon, P.A.F., Del-Rei, R.P., Krieger, M.A., Gomes, Y.M., 2018b. Am. J. Trop. Med. Hyg. 99, 1174–1179.
Santos, C.C., Pimenta, T.C., Thomasini, R.L., Verly, R.M., Franco, D.L., Ferreira, L.F., 2019. J. Electroanal. Chem. 846, 113163.
Selvapandiyan, A., Croft, S.L., Rijal, S., Nakhasi, H.L., Ganguly, N.K., 2019. PLoS Neglected Trop. Dis. 13, e0007616.
Srivastava, P., Dayama, A., Mehrotra, S., Sundar, S., 2011. Trans. R. Soc. Trop. Med. Hyg. 105, 1–6.
Steverding, D., 2017. Parasit. vectors 10, 82.
Swets, J.A., 1988. Science 240, 1285–1293.
Zhang, T., Xing, B., Han, Q., Lei, Y., Wu, D., Ren, X., Wei, Q., 2018. Anal. Chim. Acta 1032, 114–121.